Chapter 6
Modelling of Hydrodynamics and Salinity Characteristics in Chilika Lagoon

R. S. Kankara and U. S. Panda

Abstract Hydrodynamic circulation is a primary factor for most of the physical and ecological processes in lagoon environments. Chilika – Asia's largest brackish water lagoon is experiencing signficant transformations such as siltation, the growth of invasive macrophytes, northward migration of mouth and choking of the outer channel. These transformations are responsible for the reduced salinity, reduced water depth and weak lagoon-sea interaction, which in turn has led to decline in water spread area, increase in vegetated area and decrease in fish productivity. Chilika Development Authority (CDA) has taken up various initiatives to maintain the lagoon environment including improvement of Chilika mouth. Modelling is a useful tool to understand the influx of tides, wind stress and impact of freshwater influx into the lagoon and to analyse the hydrodynamic processes based on 'what if' scenario. A two-dimensional hydrodynamic model has been setup to investigate the changes in the hydrodynamics and salinity regime of the lagoon during the pre (1999) and post (2009) hydrological intervention period as well as the present scenario (2015). The study suggests that post-intervention period has significantly improved the lagoon-sea fluxes, seawater ingress and flushing of flood waters. With the advance of freshwater discharge during monsoon and post-monsoon, the mean salinity levels increased from 2.87 to 4.87 psu during 1999–2009 period, and subsequently reduced to the 3.4 psu in 2015.With all forcing factors, the annual increase in the mean salinity distribution during 2009 is 36% which has reduced to 18% in 2015. The increases in salinity underpin enhancement in several wetland ecosystem services and livelihood benefits to communities living in and around the lagoon. Reduction in salinity in later periods points to the need to maintain the inlets and dredged channels for sustainable management of the lagoon ecosystem.

Keywords Hydrodynamics · Salinity · Tidal exchange · Modelling · MIKE-21

R. S. Kankara (✉) · U. S. Panda
National Center for Coastal Research (NCCR), Ministry of Earth Sciences, Chennai, India
e-mail: kankara@nccr.gov.in

C. M. Finlayson et al. (eds.), *Ecology, Conservation, and Restoration of Chilika Lagoon, India*, Wetlands: Ecology, Conservation and Management 6,
https://doi.org/10.1007/978-3-030-33424-6_6

6.1 Introduction

Hydrodynamic modelling in lagoon environments is a primary requirement to understand the temporal variation in physical and environmental processes that lead to ecological changes. Chilika lagoon- the most significant brackish water tropical lagoon in Asia situated in the state of Odisha, along the east coast of India (19°28′ N – 19°54′ N and 85°06′ E – 85°35′ E) and oriented in the NE-SW direction (Fig. 6.1). The lagoon is about 65 km long and 3–32 km wide, with a water spread ranging from 906 km^2 during dry season (December–June) to 1165 km^2 during rainy season (July–October). The lagoon is separated from the sea by a 60 km long sandbar, spanning 323.62 km^2 area and acting as a barrier island between the lagoon and the sea. Chilika is a shallow coastal ecosystem with an average depth of 1.5 m and the maximum depth of 4.5 m in its southern part, closer to the Kalijai temple. The lagoon exchanges seawater with the Bay of Bengal through a 25 km long shore parallel to the outer channel. The average width of the channel is 900 m, and depth is of the order of 1 m. The gradual deterioration of the inlet channel had caused a substantial reduction in the tidal prism (Chandramohan and Nayak 1994; Chandramohan et al. 2001). On the south, the lagoon is connected to Rushikulya estuary by the Palur canal. The shallow depths and shoals along the channel offer

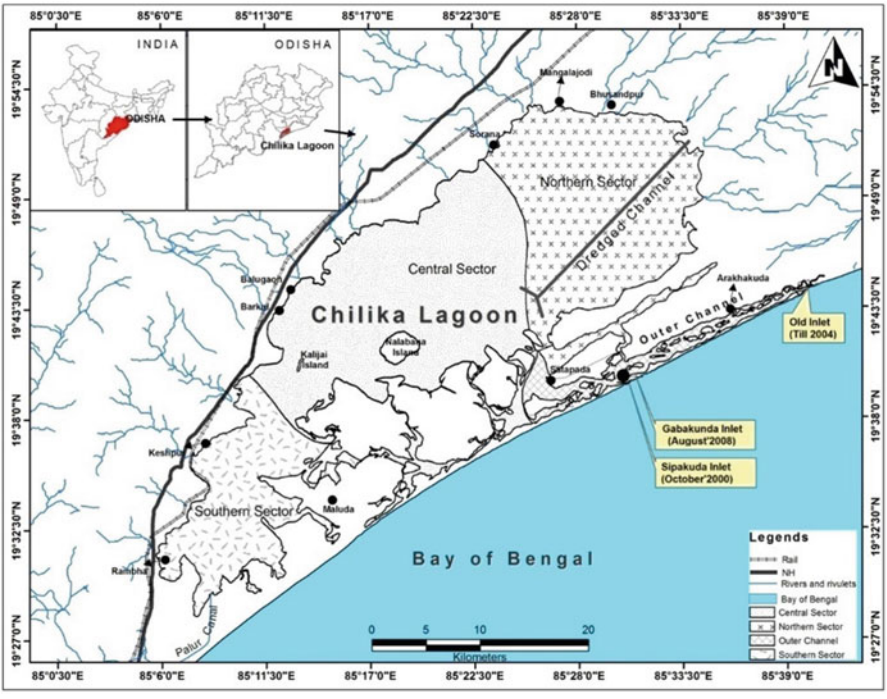

Fig. 6.1 Map of the Chilika Lagoon

considerable resistance to the flow resulting in the fall of tidal range and reduction in the tidal prism. Approximately 3.8×10^7 m^3/h of fresh water and 13 million tonnes of silt is drawn into the lagoon every year from more than 37 drains and tributaries of River Mahanadi during the monsoon season which lasts from June to September. The salinity in part of the lagoon on the northern side reduces upto 0 psu during the monsoon season due to high inflow of freshwater (Panda et al. 2015). However, the lagoon moderately regains the salinity levels during the fair weather season as a result of reduction in the discharge of fresh water into the lake and the ingress of seawater from the Bay of Bengal due to tidal circulation. About 65% of fresh water comes through Daya and Bhargavi, tributaries of river Mahanadi, which enter into the lagoon from the north (Panda 2008). The prolonged deposition of silt brought by rivers has caused the lagoon to become shallow over the years, in turn choking the Mugarmukh area, which is the the neck connecting the outer channel with the main body of the lagoon. Annual average salinity for the eastern part of the lagoon is 10–15 psu, for the central part 0.5–10 psu, and for the northern part 2–4 psu (Panda et al. 2013).

A new inlet was opened near Sipakuda in October 2000. Another channel was dredged for 200 m wide with 2.5 m depth in Magarmukh for free flow and mixing of seawater to maintain optimum salinity level inside the lagoon (CWPRS 1998). After opening of the new inlet mouth, the ecological conditions of the lagoon improved significantly (Pattnaik 2001; Mohanty et al. 2009). But, over the years, it has been observed that the inlet has migrated towards the north,and at present, it is situated about 4 km north of the mouth location in 2000.

Selected studies are available on the historical records and migration of Chilika inlets (Panda et al. 2013; Mishra and Jena 2014). Littoral drift and continuous deficient runoff of the Mahanadi basin for 2–3 years has helped forming large ebb deltas on both faces of the tidal inlet, inducing its closure. The tidal inlets of Chilika Lagoon are influenced by micro-tidal waves and the fine grained sandy coast with steeper slopes in north flank than the south. Sediment transport occurs in the surf zone, moving parallel to the coast. A part of the sediment gets deposited on the shore. Deposition is primarily due to the oblique waves breaking near the shore. Storm surges overtop and overwash a large quantum of water laden with sediment from Bay of the Bengal to the back barrier lagoon. After each storm, the evacuation of that volume through the channel section slows down. Consequently, the channel section either closes or shifts. The longshore transport is accountable for the closure of an inlet. The extreme climatic events lead to fluctuations in the Chilika shoreline, and the net annual shift during 1936–2005 at the rate of 1.09 m towards the Bay of Bengal (Mishra and Jena 2014).

Mathematical modelling is a useful tool to understand the existing hydrodynamic conditions of the Chilika lagoon, and to predict different scenarios for Chilika mouth. In the present study, a two-dimensional depth-averaged hydrodynamic model was applied to Chilika lagoon (Nayak et al. 1998; Chubarenko and Tchepikova 2001; Dias and Lopes 2006; Panda et al. 2013). This model was setup to describe the hydrodynamic changes in flow and salinity Chilika lagoon for pre (1999) and post (2009) intervention and current condition (2015) periods.

6.2 Modelling Approach

6.2.1 Hydrodynamic Modelling

A state-of-the-art fully integrated with the effects of tide, winds, source/sink, and time-dependent generalised hydrodynamic model, DHI- MIKE-21, was used for two-dimensional free surface flows. The model simulated unsteady flows in one layer (vertically homogeneous) fluids and based on the numerical solution of full non-linear equations of conservation of mass and momentum integrated over the vertical to describe flow and water level variations. The effective shear stresses in the momentum equations contain momentum fluxes due to turbulence, vertical integration and subgrid-scale fluctuations are included in the model to provide damping of short-wavelength oscillations and to represent subgrid scale effects (Madsen et al. 1989; Wang 1990).The Hydrodynamic (HD) model simulates important parameters such as water elevation, current speed and directions in different space and time scale. The advection-dispersion equation solves to compute flow and distribution of salt subjected to a variety of forcing, sources and boundary conditions. Being a shallow water system with significant influence of wind, which generates good mixing between surface and sub-surface waters, it is reasonable to assume that vertical water movements are negligible and a depth-averaged model like Mike 21 can be appropriate. Many researchers also justified the use of a two-dimensional vertically integrated model with respect to approaches that consider two or more vertical layers in the absence of stratification phenomena (Ramirez and Imberger 2002; Balas and Özhan 2002; Zacharias and Gianni 2008).The hydrodynamics of such a lagoon can be described by using a well known shallow water equations, which describe the evolution of an incompressible fluid in response to gravitational and rotational accelerations (Pedlosky 1987) and mass transport equation for salinity.

Shallow water equations for hydrodynamics: Integration of the continuity and horizontal momentum equations over depth requires the following two-dimensional shallow water equations (DHI 2007).

$$h = \eta + d$$

$$\frac{\partial h}{dt} + \frac{\partial h\overline{u}}{dx} + \frac{\partial h\overline{v}}{dy} = hS$$

$$\frac{\partial h\overline{u}}{dt} + \frac{\partial h\overline{u}^2}{dk} + \frac{\partial h\overline{uv}}{dy} = f\overline{v}h - gh\frac{\partial \eta}{dx} - \frac{h}{\rho_0}\frac{\partial p_a}{dx} - \frac{gh^2}{2\rho_0}\frac{\partial \rho}{\partial x}$$
$$+ \frac{\tau_{sx}}{\rho_0} - \frac{\tau_{bx}}{\rho_0} - \frac{1}{\rho_0}\left(\frac{\partial s_{xx}}{\partial x} + \frac{\partial s_{xy}}{\partial y}\right) + \frac{\partial}{\partial x}(hT_{xx}) + \frac{\partial}{\partial y}(hT_{xy}) + hu_sS$$

$$\frac{\partial h\overline{v}}{dt} + \frac{\partial h\overline{uv}}{dx} + \frac{\partial h\overline{v}^2}{dy} = -f\overline{u}h - gh\frac{\partial \eta}{dy} - \frac{h}{\rho_0}\frac{\partial p_a}{dy} - \frac{gh^2}{2\rho_0}\frac{\partial \rho}{\partial y}$$
$$+ \frac{\tau_{sy}}{\rho_0} - \frac{\tau_{by}}{\rho_0} - \frac{1}{\rho_0}\left(\frac{\partial s_{yx}}{\partial x} + \frac{\partial s_{yy}}{\partial y}\right) + \frac{\partial}{\partial x}(hT_{xy}) + \frac{\partial}{\partial y}(hT_{yy}) + hu_sS$$

Where, t is the time (s); x and y are the Cartesian co-ordinates (m); η is the surface elevation; d is the still water depth (m); $(h = \eta + d)$ is the total water depth (m); $\overline{u}$ and $\overline{v}$ are the depth averaged velocity components in the x and $y$directions; $f = 2\Omega \sin \varphi$ is the Coriolis parameter, Ω is the angular rate of revolution and φ the geographic latitude; g is the gravitational acceleration;ρ is the density of water; s_{xx}, s_{xy}, s_{yx} and s_{yy} are components of the radiation stress tensor; T_{xx}, T_{xy}, T_{yx} and T_{yy} are components of lateral stress; τ_{sx} and τ_{sy} are the components of the surface wind stress; τ_{bx} and τ_{by} are the components of bottom stress; p_a is the atmospheric pressure; ρ_0 is the reference density of water; ρ is the density of water; S is the magnitude of the discharge due to point sources; u_s and v_s are the velocity by which the water is discharged into the ambient water. The lateral T_{ij} includes viscous friction, turbulent friction and differential advection. They are estimated using an eddy viscosity formulation based on the depth averaged velocity gradients

$$T_{xx} = 2A\frac{\partial \overline{u}}{\partial x}, T_{xy} = A\left(\frac{\partial \overline{u}}{\partial y} + \frac{\partial \overline{v}}{\partial x}\right), T_{yy} = 2A\frac{\partial \overline{v}}{\partial y}$$

6.2.1.1 Mass Transport Equations for Salinity

The transports of temperature, T, and salinity, s, follow the general transport-diffusion equations as $\frac{\partial s}{dt} + \frac{\partial us}{dx} + \frac{\partial vs}{dy} + \frac{\partial ws}{dz} = F_s + \frac{\partial}{dz}\left(D_v \frac{\partial T}{dz}\right) + s_s S$.

Where, D_v is the vertical turbulent (eddy) diffusion coefficient, $\widehat{H}$ is a source term due to heat exchange with the atmosphere, and T_s and s_s are the temperature and the salinity of the source.

6.2.1.2 Bottom Stress

The bottom friction can be specified as the frictional velocity associated with the bottom stress which is given by $U_{rb} = \sqrt{c_f \left|\vec{u}_b\right|^2}$. For two-dimensional calculations $\vec{u}_b$ is the depth-average velocity and the drag coefficient can be determined from the Chezy number, $C\ (m^{1/2}/s)$. The specified values for the Chilika environment for Chezy number is 32 and a constant eddy viscosity of 0.5 m^2/s is used (Chapra 1997).

The spatial discretisation of equations is performed using a cell-centred finite volume method in the horizontal plane an unstructured grid is used comprising of triangle elements. An approximate Riemann solver is used for convective fluxes, which makes it possible to handle the discontinuous solutions. For the time integration, an explicit Euler method is used. Due to the stability restriction using an explicit scheme, the time step interval should be selected so that the Courant-Friendrich-Levy (CFL) number is less than 1. For the present study CFL number less than the critical CFL number (0.8) has been observed. The approach for treatment of the moving boundaries problem (flooding and drying fronts) is based on the work by

(Zhao et al. 1994). The depth of each cell is monitored, and the cells are classified as dry, partially dry or wet and flooded boundaries. As the Chilika lagoon is very shallow, the values considered for drying depth $h_{dry} = 0.005$ m, flooding depth $h_{flood} = 0.05$ m and wetting depth $h_{wet} = 0.1$ m which satisfy the rule $h_{dry} < h_{flood} < h_{wet}$.

6.2.2 *Model Domain and Bathymetry*

The numerical computation has been carried out on a spatial domain that represents the Chilika lagoon through an unstructured mesh. It allows high flexibility with its subdivision of the numericaldomain varying in form and size. It is especially suited to reproduce the geometry and the hydrodynamics of complex shallow water basins such as the Chilika lagoon with its narrow outer channel area, small islands, dredged channels and uneven complex boundary structure. Two model domains were generated from 85°04′ to 85°43′ East and 19°27′ to 19°55′ North coordinates, based on the information from British Admiralty Sea Maps (extracted from a DHI C-MAP in digital form), and toposheets of Chilika region prepared by the Survey of India and from various field observations. The bathymetry map has been validated with the GPS observations collected during field survey. The mesh files for the Chilika lagoon, pre-intervention period i.e., for the year 1999 (Fig. 6.2a, Domain 1: 7440 nodes and 7278 elements) and post-intervention period i.e., for the year 2009 (Fig. 6.2b, Domain 2: 3542 nodes and 5231 elements) and current condition i.e., year 2015 (Fig. 6.2c, Domain 3: 4084 nodes and 6112 elements) has been configured considering the computational unstructured mesh, water depths and boundary information. Subdivision of the continuum discretizes the spatial domain into

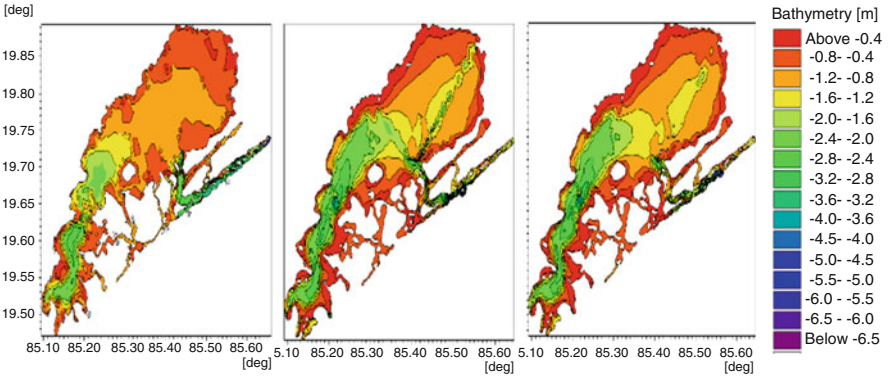

Fig. 6.2 Model domains for (**a**) pre-intervention (**b**) post-intervention and (**c**) present condition period

non-overlapping cells/elements. In the two-dimensional case the elements can be arbitrarily shaped polygons, however, in this study, only equilateral triangles were considered.

Large angles and high resolutions in a mesh contradict with the need for short simulation times. The resolution of the mesh, combined with the water depths and chosen time-step governs the Courant numbers in a model set-up. The maximum Courant number maintained to be less than 0.5. Such that simulation time dependency on the triangulation of the mesh relates not only to the number of nodes in the mesh, but also the resulting Courant numbers. The Courant number C_R expresses the number of computational points the information moves in one time step. $C_R = c\frac{\Delta t}{\Delta x}$. Where, c (celerity) $=\sqrt{gh}$, Δt is t time step and Δx is the grid spacing. As a result of this, the effect on simulation time of a fine resolution at deep water can be relatively high compared to a high resolution at shallow water.

6.2.3 Model Setup

Chilika is mainly influenced by tides, wind and fresh water inflow, therefore waves have been omitted in simulation. However, flooding and drying in shallow areas were considered to obtain accurate results, as model domain covers vast shallow patches. Total 4084, 6012 nodes were generated in the lagoon to represent the pre and post intervention bathymetry. The drying depth (minimum water depth allowed in a point before being taken out of calculation) was set at 0.01 m, and the flooding depth (water depth at which the point will be re-entered into the calculation) was set to 0.05 m. The model computational time step was set to 300 seconds and simulations were carried out for 28,800 time steps with CFL number less than 0.8. Considering the facts that Chilika receives considerable freshwater only in monsoon from 19 source points, the estimated quantity of fresh water was introduced during July–October, and negligible flux was imposed during fair season simulations. In the beginning, the seais set at rest by providing a constant water level uniformly in the model domain (i.e. z = 1.31 m, u = v = 0 att = 0) as an initial condition. Time series hourly data of water level was imposed at open sea boundary, i.e., at the mouth. Several short simulations were carried out toperformseveral sensitivity runs and tuning the calibration parameters (Chezy number (C) and Eddy viscosity) in order to develop confidence in ‘what if ‘scenario assessments. During the calibration, the hydrodynamic and water quality parameters were adjusted to get a satisfactory correspondence between model results and observed field data.To quantify the agreement between model and observations, method proposed by Willmott (1981) was used. Model was setup for 1 year for 3 different conditions year 1999, 2009 and 2015 corresponding to pre-intervention, post-intervention and current period, with three distinct forcing combinations i.e., (a) tide only, (b) tide + wind and (c) tide + wind + freshwater discharge. Finally, the model was run for 21 Dec 1998 to 31 Dec 1999, 21 Dec 2008 to 10 Nov 2009 and 21 Dec 2014 to 10 Nov 2015.

6.3 Results and Discussion

6.3.1 Water Level

The model was simulated for a 330–380 days period with initial and boundary conditions. Water level and flux at each nodal point were computed for each time step. Hourly time series data were stored to analyse the model results. Results of water level indicate the tendency of decreasing tidal amplitudes from the inlet mouth towards the Satpada. The model was able to capture the impact of the intervention on the water level. The simulated tidal range was 2.2 m at Sipakuda inlet, 0.7 at Satpada, 0.2–0.4 m in the main body of the lagoon during post-intervention period (2009) in comparison to significantly lower ranges of 0.4 m at Sipakuda, 0.2–0.3 m at Satpada and 0.1–0.2 in the main body of the lagoon during the pre-intervention period (1999). It may be noted that the major tidal variation was in the channel between Arakhakuda (Old inlet) upto Sipakuda during pre-intervention period. Water levels (near inlet) shows that the tidal amplitude is maximum at the inlet of the lagoon which decreases gradually as we proceed inward from the inlet, while the astronomical tidal range at inlet matched with observed data, at remote locations in the main body of the lagoon.

The model results were validated with field measurements (water level at Inlet, near Nalabana representing the central sector, on the lead channel representing the northern sector and near INS Chilika representing the southern sector) for the simulation period. Simulation of water levels (Fig. 6.3) shows that the tidal amplitude is maximum at the inlet which decreases gradually as we proceed inward from the inlet. The lunar principal constituent M2, observed to be dominant at Sipakuda inlet also the 'form number' depicts the semi-diurnal nature of the tide near the inlet. The M2 represents the tide due to a fictitious moon circling the equator at the mean lunar distance and with constant speed. Harmonic analyses made for four locations covering inlet and three sectors determined the tidal constituents (Amplitude and phase). Tide near inlets are purely semi-diurnal micro tide having tidal form number 0.18 and mixed semi-diurnal during monsoon with the tidal form number 0.30. The tides transform into mixed mainly semi-diurnal inside the lagoon, primarily when the complex bottom topography inside the shallow lagoon and dry period reduces the semi-diurnal component amplitudes through friction and non-linear effects (Dias 2001).

Figure 6.4 shows the hourly water level profile for a tidal cycle across the lagoon at six locations form Sipakuda>Satapada>Mugarmukha>central sector and two representative locations at centre of northern and southern sectors during post monsoon period. It is clearly seen that the water level of main lagoon are is much lower than outer channel region. A steep gradient from Sipakuda to Muggarmukha was also observed, which generates higher current velocity. During 1999–2009 period, the water level increased on an average by 20 cm, but the increase in 2015 was only marginal. (~5 cm).

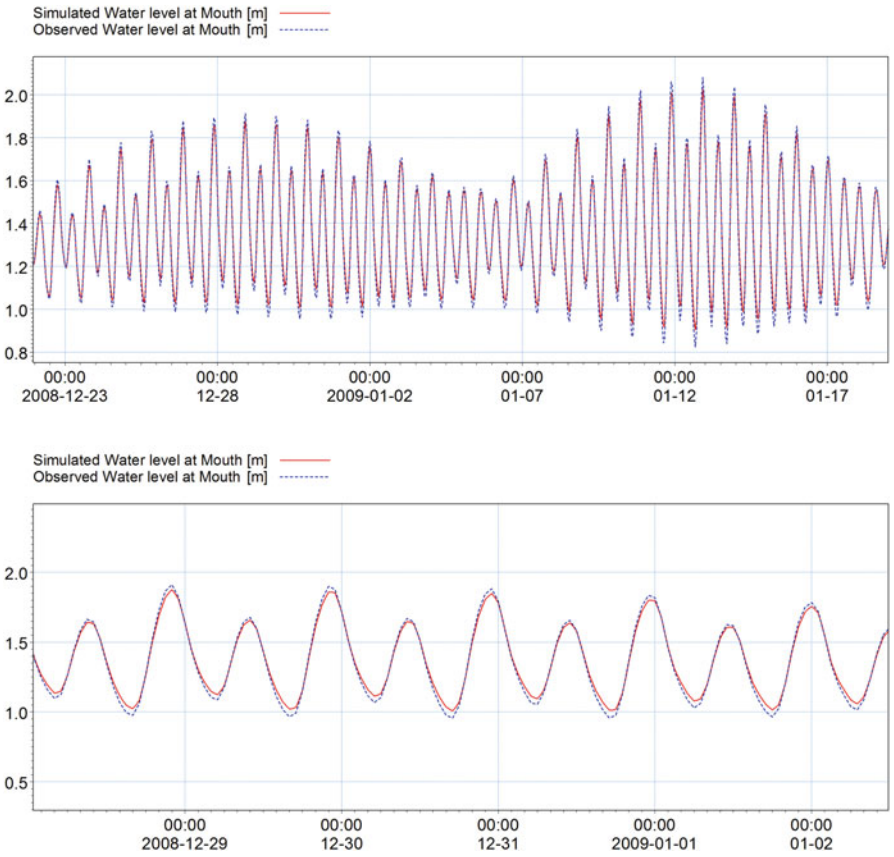

Fig. 6.3 Validation of water levels between Sipakuda inlet and Satapada during post intervention period (2009)

6.3.2 Surface Water Circulation

Hydrodynamics of the lagoon is governed by many forcing like bathymetry, wind stress, tides and freshwater influx from the rivers. In Chilika, wind-driven circulation dominates the density-driven circulation (Mohanty and Panda 2009). Due to the large open surface, the wind is a significant forcing factor in stimulating circulation. Seasonal changes in the wind magnitude and direction can cause large-scale changes in the circulation pattern of the lagoon. Apart from such seasonal changes, land and sea breeze, also affects the circulation in the lagoon. The role of wind in generating turbulence is more important in the lagoon zones distant from the sea, where tide-induced flows have no relevance (Cioffi et al. 1995). Apart from the surface wind stress, bottom topography and bathymetry is another crucial factor controlling the circulatory pattern in shallow lagoons. Tidal influx causes major changes in the

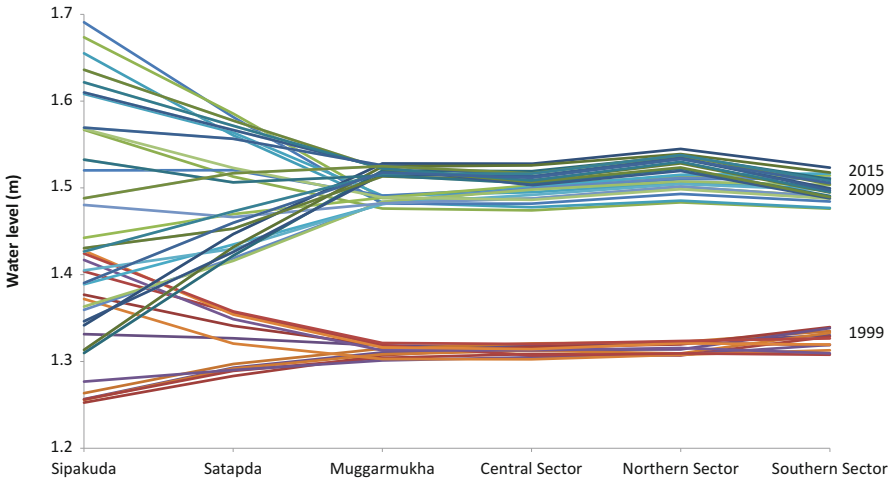

Fig. 6.4 Simulated hourly water level profiles from Sipakuda inlet towards the main body of the lagoon over period of 12 h

circulation in lagoonsbut its effect is limited to the region near the tidal inlet. Circulation in lagoon is also influenced by freshwater influx.

From the hydrodynamic simulations, it is seen that tide generated currentsbegin from the inlet of Chilika, crosses over the Muggarmukh channel and reach main body of the lagoon. The primary direction groups are easterly and westerly directions along the Outer Channel orientations. The current speed has significantly increased to the order of 30–40% at outer channel region with the intervention resulting in a better influx of seawater. Consequently, the saline water easily propagates in the main body of the lagoon. Simulated current velocity was observed to be maximum at inlet (0.5 m/s) and lower in the other parts of the lagoon (0.02–0.05 m/s). A significant portion of waters moves towards southern sector through the central sector with a speed of 0.04–0.06 m/s (Fig. 6.5).

Interestingly, eddies were observed in the northern sector and southern sector. During monsoon, water currents are higher in northern sector due to runoff than the southern sector. Flood currents could be seen between Muggarmukha to Satapada channel areas, which gradually decreases towards the main body of the lagoon. In the post-intervention period, the floodwaters were observed to enter into the lagoon through the Muggarmukha channel and diverges into two streams, one towards southern sector through central sector, and other towards northern sector, especially along the lead. Further, the northern sector stream diverges into to two parts and forms eddy like circulation pattern in its western and eastern parts (Fig. 6.5). Circulation patterns in the northern sector indicate the predominant role of the bottom topography.

The hydrodynamic simulations affirm the primal role of wind as the primary forcing factor on the water circulation in the main body of the lagoon. The tide determines the discharges through the connecting inlet and modulates the circulation

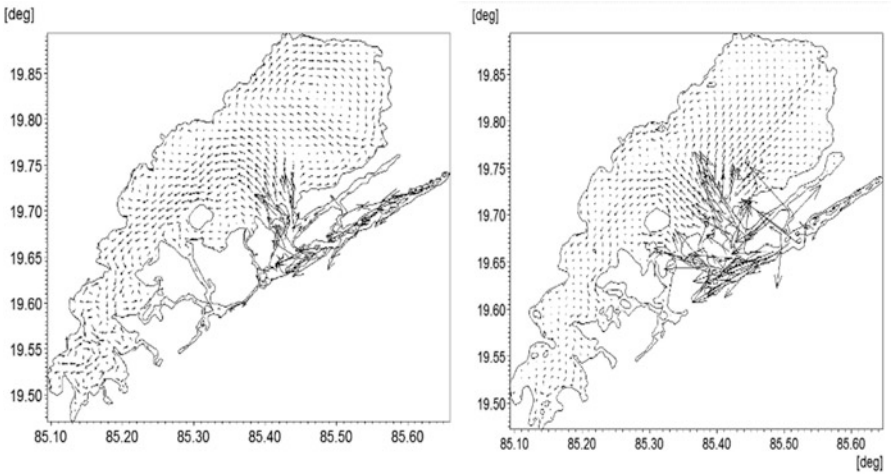

Fig. 6.5 Simulated flood current pattern during January (**a**) 1999 (pre-intervention) and (**b**) 2009 (post-intervention)

pattern set up by the wind. Topographies of the bottom along with width are responsible for the formation of gyre circulation subsystems in the north sector and some parts of the southernsector. However, with substantial freshwater influx after monsoon drives the water in unidirectional towards the sea through the inlet and changes the entire circulation pattern.

6.3.3 Salinity Simulation

Salinity was simulated by prescribing concentration at the inlet and zero concentration at 19 source points. Salinity pattern drives the lagoon ecosystem. Spatial-temporal variation of salinity in the lagoon is significant, ranging from fresh water regime (~5) to saline regime (~35) during the summer; whereas it reduced to entirely fresh in northern sector to brackish (~10) in the main body of the lagoon during wet period due to massive influx of freshwater discharge into the lagoon. The lagoon is well mixed in a vertical column and has negligible salinity stratification. Salinity gradient is lower in the southern sector and gradually increases in the direction of lagoon inlet (Panda and Mohanty 2008). For salinity simulation, a number of simulation scenarios were executed using different combinations of the four calibration factors in Dalton's and Angstrom's law (Zacharias and Gianni 2008) run,and the model sensitivity to each of the constants was checked out. Latent heat flux, wind coefficient and sun constants were calibrated for the regions. The shortwave penetration is dependent on the visibility, which has been specified with one as a light extinction coefficient. The heat exchange is included with air temperature, relative humidity and clearness coefficient. European Centre for Medium-Range Weather

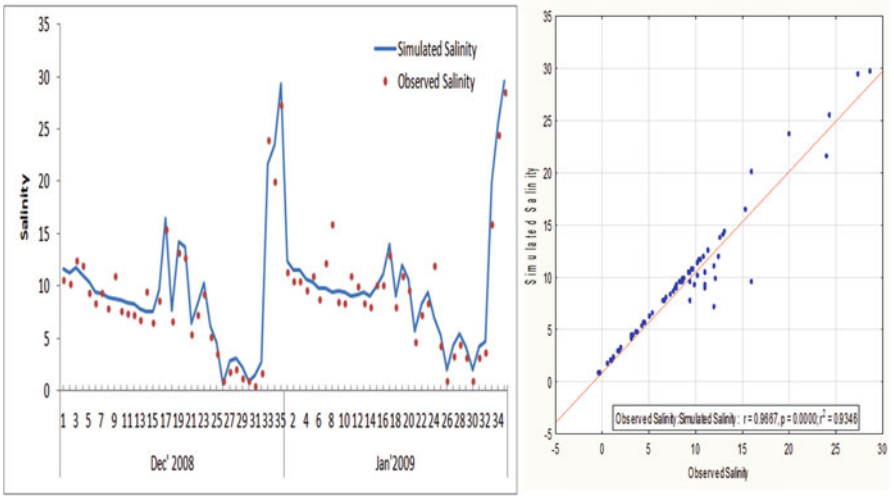

Fig. 6.6 (**a**) Validation of Salinity at 36 stations uniformly distributed over the lagoon (**b**) Regression analysis between observed and simulated salinity for the 36 locations

Forecasts (ECMRWF) data for 1999 and 2015 and AWS measurements (IMD) for 2019 were used. The initial conditions were defined with a surface distribution from various measurements.

Simulations are performed to understand and quantify different forcing factors – wind, tides and freshwater discharge – and their independent and combined roles in the hydrodynamics and salinity distribution in the lagoon. The results indicate that the signatures of salinity intrusion through inlet, low salinity in northern sector, and medium salinity in southernsector. Salinity validation made at 36 stations for the exact time of sampling (stations uniformly distributed over whole lagoon) during post-intervention period (2009) agrees well with observation with $r^2 = 0.93$ (Fig. 6.6). Results suggest that the temporal variability is mainly due to the disparity of the seasonal changes in salinity (Fig. 6.7).

The time series data indicates a significant increase in salinity during post-intervention periods. Experiments with tidal forcing alone show that tides have transported salinity in the channel upto the Muggurmukh (gut area) (Fig. 6.8). The wind forcing affects salinity redistribution mostly in the main body of the lagoon. The opening of the inlet at Satapara has helped in increasing the tidal influx and hence the salinity, the influence is visible in the main body of the lagoon (Figs. 6.9a and 6.9b). The month of June is the transition period for a change in salinity, being linked with the onset of monsoonal precipitations and consequently substantial freshwater influx into the lagoon. The simulations indicate that the the lagoon takes nearly 6–8 weeks to restore the salinity regime after the monsoonal flood.

The variation of mean salinity with the engineering interventions during October 2000 is shown in Table 6.1. It is noted that after the hydrological intervention, the influx of seawaterhas improved the salinity distribution in the lagoon. During

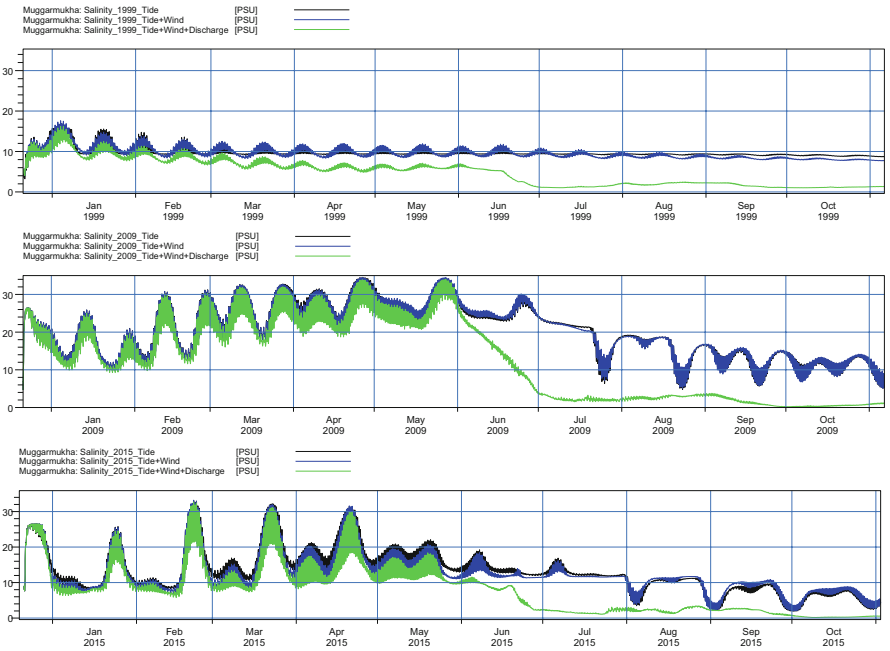

Fig. 6.7 Seasonal and annual mean salinity variation in pre- (1999) and post- (2009) interventions and current situation (2015) period with combinations of different forcing factors (Tide only, Tide + Wind and Tide + Wind + Freshwater discharge)

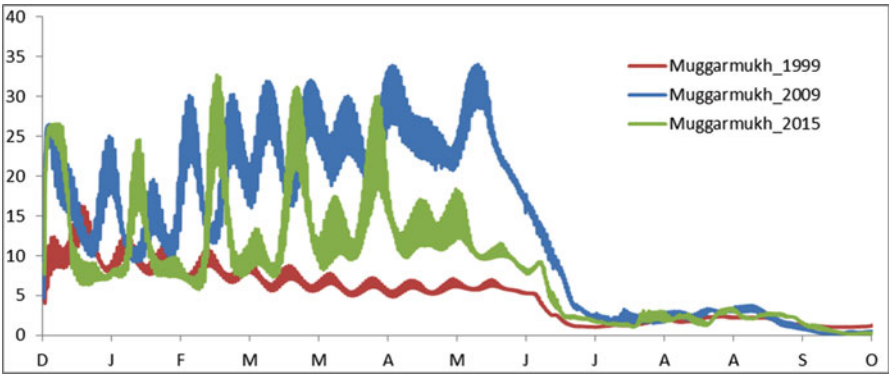

Fig. 6.8 Mean salinity at profile at Muggarmukh during pre- (1999) and post- (2009) interventions and current situation (2015)

summer (March–June), mean salinity has increased from ~6 psu in 1999 to ~17 psu in 2009 (163%), dipping to ~12 psu in 2015. In monsoon (July–Oct) with freshwater influx, salinity increased by 147% during 1999–2009, and 111% during 1999–2015. A similar pattern was observed during the post-monsoon period with tide and tide + wind forcing.

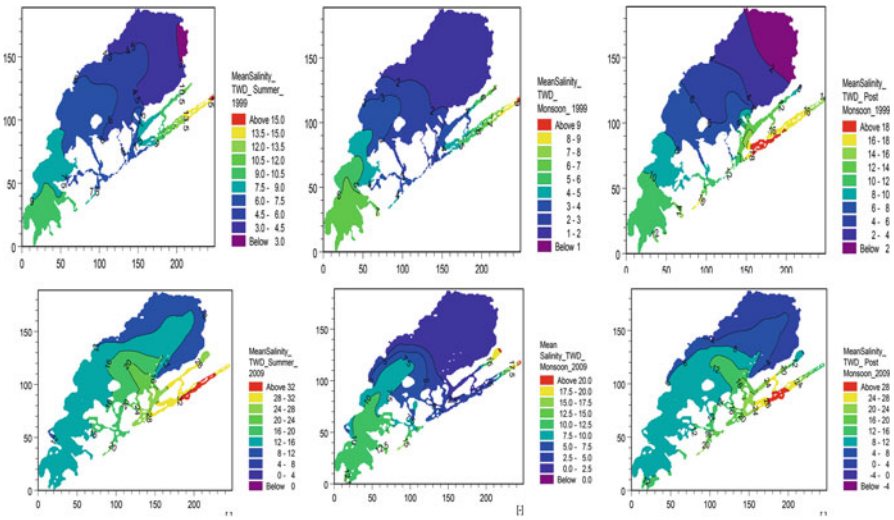

Fig. 6.9a Spatial variation of seasonal mean salinity during pre- (1999) and post- (2009) interventions with Tide + Wind + Freshwater discharge forcing

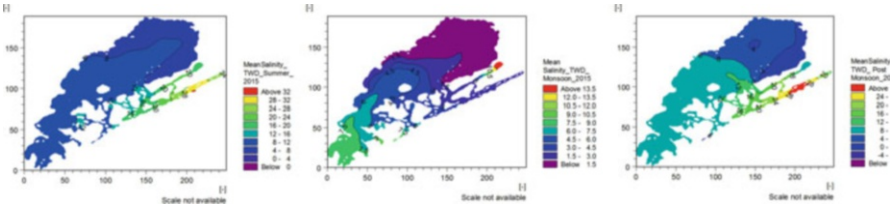

Fig. 6.9b Spatial variation of seasonal mean salinity during current situation (2015) period with Tide + Wind + Freshwater discharge forcing

The freshwater discharge has completely altered the lagoon's ecosystem. With the advance of freshwater discharge during monsoon and post-monsoon, the modelled mean salinity falls upto 2.87 psu, 4.87 psu and 3.4 psu in 1999, 2009 and 2015.Thisindicates reduced flushing of freshwater into the sea during 2009–2015 period.

However, during post-monsoon, the freshwater discharge continues and still decreases the salinity improvement at 41% even though the mean salinity increased nearly two-fold during the monsoon period. When modelled with all forcing factors, annual salinity was observed to increase by 36% during 1999–2009 period, however,reduced to 18% in 2015.

Comparing the salinity profiles in three periods (Fig. 6.8), it is clear that the hydrological intervention has led to improvement in salinity the regimes. The spatial mean salinity figures also reveal the same. The higher isohalines in the lagoon, especially in the northern sector, depicts the role of dredged mouth and lead channel which provides a clear passage for seawater into the lagoon (Fig. 6.9b). The funnel

Table 6.1 Seasonal and annual mean salinity variation in psu in pre- (1999) and post- (2009) interventions period with different forcing factors

Forcing factors	Season	Pre-intervention (1999)	Post-intervention (2009)	Current condition (2015)	Change in mean salinity 1999–2009 (%)	Change in mean salinity 2009–2015 (%)
Tide only	Summer (MAMJ)	6.64	17.43	12.02	163	132(−31)
	Monsoon (JASO)	6.8	16.81	10.78	147	111(−36)
	Post Monsoon (NDJF)	6.4	9.34	9.37	46	0
	Annual	3.79	8.53	6.64	125	123(−22)
Tide + Wind	Summer (MAMJ)	6.73	17.8	12.48	164	134(−30)
	Monsoon (JASO)	6.93	17.03	11.18	146	112(−34)
	Post Monsoon (NDJF)	6.44	9.35	9.54	45	47(+2)
	Annual	4.09	8.63	6.64	111	88(−23)
Tide + Wind + Freshwater Discharge	Summer (MAMJ)	6.1	15.09	10.37	147	116(−31)
	Monsoon (JASO)	2.87	4.87	3.4	70	40(−30)
	Post Monsoon (NDJF)	6.32	8.91	9.08	41	43(+2)
	Annual	4.14	5.65	4.64	36	18(−18)

type isohalines from Muggermukh towards the central sector and further higher gradient isohalines towards southern sectorshows the improvement in the brackish water characteristics of the lagoon during post-intervention (2009) period. In 2015, however, salinity has been observed to decline.

6.4 Conclusion

The two-dimensional hydrodynamic model was used to obtain nine synoptic views of hydrodynamic and salinity pattern for Chilika lagoon for three scenarios (1999, 2009 and 2015) and three significant forcings (tide, wind and freshwater influx). The model results are promising for simulating spatial variations of hydrodynamic propagation, and salinity conditions in response to multiple forcing mechanisms. It is concluded that the tide and wind are the primary forcing factor during the summer

period, whereas freshwater influx during monsoon and post seasons influences the water mass and circulation. Wind is responsible for the formation of clockwise and counter-clockwise circulation subsystems in the main body of the lagoon. With monsoon onset, substantial freshwater inflow to the lagoon drives the water unidirectional towards the sea and alters the whole circulation pattern. Inlet and upland discharge control the salinity regime. Salinity gradients are diverse with different water masses of the lagoon, however, after monsoon lagoon tends to the freshwater regime. Hydrological intervention and concurrent restoration measures have facilitated better exchange with sea resulting in an improvement in salinity distribution and hence ecology of the lagoon. Shifting of the inlet(s) and siltation in the dredged channels are significant concerns, which has slowly trending lower saline influx in post-intervention to present conditions. The inlet is highly dynamics over a period of time and depends on freshwater discharge and northward longshore drift along the coastline. The present scenario of lagoon system suggests detailing modelling of the lagoon by incorporating the latest bathymetry, geomorphologic features around the inlet, flushing/dredged channels and Muggarmukh gut area.

References

Balas L, Özhan E (2002) Three-dimensional modelling of stratified coastal waters. Estuar Coast Shelf Sci 54:75–87. https://doi.org/10.1006/ecss.2001.0832

Chandramohan P, Nayak B (1994) A study for the improvement of the Chilka Lake tidal inlet, East Coast of India. J Coast Res 10:909–918

Chandramohan P, Jena B, Kumar V (2001) Littoral drift sources and sinks along the Indian coast. Curr Sci 81:292–297

Chapra S (1997) Surface water-quality modeling. Tufts University/Waveland Press, Inc, Illinois

Chubarenko I, Tchepikova I (2001) Modelling of man-made contribution to salinity increase into the Vistula Lagoon (Baltic Sea). Ecol Model 138:87–100. https://doi.org/10.1016/S0304-3800(00)00395-1

Cioffi F, Eugenio A, Gallerano F (1995) A new representation of anoxic crises in hypertrophic lagoons. Appl Math Model 19:685–695

CWPRS (1998) Mathematical model studies to assess the effect of the proposed channel flow circulation and salinity Chilika Lake, Odisha. Pune

DHI (2007) Mike21 & Mike 3 flow model FM. Hydrodynamic and transport module: scientific documentation

Dias J (2001) Contribution to the study of the Ria de Aveiro hydrodynamics. University of Aveiro, Aveiro

Dias J, Lopes J (2006) Implementation and assessment of hydrodynamic, salt and heat transport models: the case of Ria de Aveiro Lagoon (Portugal). Environ Model Softw 21:1–15

Madsen P, Rugbjerg M, Warren I (1989) Subgrid modelling in depth integrated flows. In: 21st international conference on coastal engineering. American Society of Civil Engineers, Spain, pp 505–511

Mishra S, Jena J (2014) Migration of tidal inlets of Chilika Lagoon, Odisha, India – a critical study. Int J Eng Technol 6:2453–2464

Mohanty P, Panda U (2009) Circulation and mixing processes in Chilika lagoon. Indian J Geo-Mar Sci 38:205–214

Mohanty R, Mohapatra A, Mohanty S (2009) Assessment of the impacts of a new artificial lake mouth on the hydrobiology and fisheries of Chilika Lake, India. Lakes Reserv Res Manag 14:231–245. https://doi.org/10.1111/j.1440-1770.2009.00406.x

Nayak B, Ghosh L, Roy S, Kankara R (1998) A study on hydrodynamics and salinity in the Chilika Lake. In: International workshop on sustainable development of Chilika Lagoon. Chilika Development Authority, Bhubaneshwar, pp 31–47

Panda U (2008) Modelling water quality and spatial information system on Chilika Lagoon. Berhampur University

Panda U, Mohanty P (2008) Monitoring and modelling of Chilika environment using remote sensing data. In: Sengupta M, Dalwani R (eds) Taal2007: the 12th world lake conference, Jaipur, pp 617–638

Panda U, Mohanty P, Samal R (2013) Impact of tidal inlet and its geomorphological changes on lagoon environment: a numerical model study. Estuar Coast Shelf Sci 116:29–40. https://doi.org/10.1016/j.ecss.2012.06.011

Panda U, Mahanty M, Rao V et al (2015) Hydrodynamics and water quality in Chilika Lagoon-a modelling approach. Procedia Eng 116:639–646

Pattnaik A (2001) Hydrological intervention for restoration of Chilika Lagoon. In: Chilika newsletter, vol 2. Chilika Development Authority and Wetlands International South Asia, pp 3–5

Pedlosky J (1987) Geophysical fluid dynamics, 2nd edn. Springer, New York

Ramirez I, Imberger J (2002) The numerical simulation of the hydrodynamics of Barbamarco Lagoon, Italy. Appl Numer Math 40:273–289

Wang J (1990) Numerical modelling of bay circulation. In: Méhauté B, Hanes D (eds) The sea: ocean engineering science. Wiley, New York, pp 1033–1066

Willmott C (1981) On the validation of models. Phys Geogr 2:184–194

Zacharias I, Gianni A (2008) Hydrodynamic and dispersion modeling as a tool for restoration of coastal ecosystems. Application to a re-flooded lagoon. Environ Model Softw 23:751–767

Zhao D, Shen H, Tabios G et al (1994) Finite-volume two-dimensional unsteady-flow model for river basins. J Hydraul Eng 120:863–883. https://doi.org/10.1061/(ASCE)0733-9429(1994)120:7(863)